Simulations Exploring the Dependence of Cloud-Cover Frequency Distribution on Cloud Size and Image Pixel Resolution

GANG LUO

UCAR Visiting Scientist Program, NOAA Science Center, Washington, DC

(Manuscript received 18 March 1994, in final form 5 December 1994)

ABSTRACT

The dependence of pixel-scale cloud-cover frequency distribution on cloud size and pixel size is examined through Monte Carlo simulations. A shape parameter, which describes the shape of the frequency distribution, is found to be a simple function of the ratio of cloud size to pixel size. The form of the frequency distribution changes from U shape to bell shape when the ratio decreases. It becomes uniform when the ratio is about 0.8–0.9 for the cases where the regional-scale cloud cover is 0.5. It is shown that on average the cloud cover in partially cloudy pixels increases with increasing regional-scale cloud cover when the ratio of cloud size to pixel size is small. It becomes insensitive to regional-scale cloud cover when the ratio becomes large. It is also shown that, in comparison with the results from Monte Carlo simulations, the grid-scale cloud-cover frequency distribution obtained using a threshold method tends to be more U shaped, and that obtained using a method that assigns 50% cloudiness to partially cloudy pixels tends to be less U shaped, particularly for subgrid cloudiness. A possible way of retrieving cloud size is suggested. It is found that the difference between a simulated cloud field, where clouds are uniformly distributed, and a real cloud field, where clouds may not be uniformly distributed, biases cloud size retrieval. Investigations on how clouds are distributed in a real cloud field are recommended.

1. Introduction

Radiative transfer in the earth–atmosphere system depends on the distribution of cloud parameters above the respective region and where cloud cover is the most popular cloud parameter (Karner and Keevallik 1993). Shenk and Solomonson (1972) simulated the dependence of the overestimation of cloud cover, obtained using a threshold, on the ratio of cloud size to satellite sensor pixel size. Falls (1974) noted that the physics of the cloud-cover variable determines the transition of a U-shaped cloud-cover frequency distribution within a small area to a bell-shaped distribution within a large area. Hughes and Henderson-Sellers (1983) analyzed the average of a cloud-cover frequency distribution as a function of the standard deviation of the cloud covers.

The intent of this paper is to examine the dependence of cloud-cover frequency distribution on cloud size and satellite image pixel resolution. Monte Carlo simulations are used to provide "true" cloud covers.

2. Description of the Monte Carlo model

The Monte Carlo model developed here is similar to that of Shenk and Solomonson (1972). As shown in Fig. 1, resolution elements are created on a two-dimensional grid, referred to as the analysis region of the model. Clouds are simulated as single-sized square arrays of resolution elements. Each resolution element is either completely within a cloud or completely cloud free. Cloud size, the length of the side of a cloud, is therefore given as an integer in the unit of the resolution element. Clouds are randomly placed in the analysis region and are allowed to overlap to build cloud clusters. In other words, cloud center points are selected from a uniform random distribution within the analysis region, making the number of cloud center points per unit area to be a Poisson distribution. The cloud cover of the resolution elements that are completely within a cloud is 1 (overcast), and that of the resolution elements that are cloud free is 0. The regional-scale cloud cover (the total cloud cover of the analysis region) is the ratio of the summation of the cloud covers of all resolution elements divided by the total number of resolution elements. The analysis region thus represents a broken cloud field containing optically opaque clouds residing in a single layer. Satellite image pixels are simulated as square arrays of resolution elements. Pixel size is the length of the side of a pixel and is given as an integer in the unit of resolution element. The cloud cover of a pixel (pixel-scale cloud cover) is accumulated from those of the resolution elements in the pixel and thus can be fractional. The normalized frequency distribution of the cloud covers of all the pixels in the analysis region is discussed in section 3. The analysis

Corresponding author address: Dr. Gang Luo, UCAR Visiting Scientist Program, NOAA Science Center, 5200 Auth Road, #711, Washington, DC 20233.
E-mail: lgang@sgi57.wwb.noaa.gov

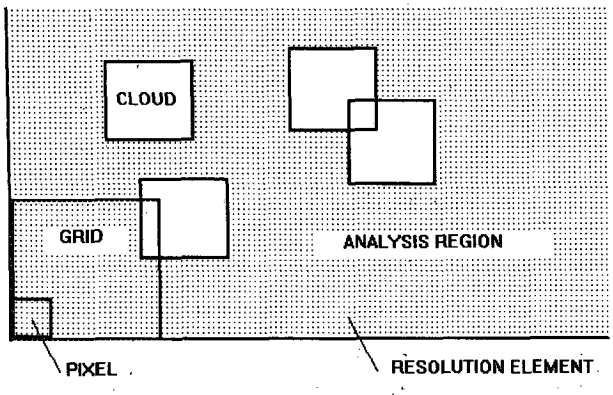

FIG. 1. A schematic plot of the simulated cloud field.

region is divided into equal-sized square grids. Grid size is the length of the side of a grid and is given as an integer in the unit of resolution element. A grid contains an array of pixels. The cloud cover of a grid (grid-scale cloud cover) is accumulated from those of the pixels in the grid. The normalized frequency distribution of the cloud covers of all the grids in the analysis region is discussed in section 4.

3. Pixel-scale cloud-cover frequency distribution

Figure 2 shows an example of the normalized frequency distribution of pixel-scale cloud covers in the analysis region. The abscissa is the cloudiness and is divided into 20 equal A_c bins, each of which spans from $(i - 1)/20$ to $(i - 1)/20 + 0.05$, where i takes the value from 1 to 20. Partially cloudy pixels are those having a cloud cover between the values of 0.05 and 0.95, while cloud-free and overcast pixels are those having a cloud cover less than 0.05 and more than 0.95, respectively. In the example shown in Fig. 2, the regional-scale cloud cover is 0.3, the cloud size is 60, and the pixel size is 20. The distribution is U shaped, since the cloud size is larger than the pixel size, as noted by Falls (1974). When the cloud size is smaller than the pixel size, the distribution will be bell shaped. In addition, when the regional-scale cloud cover is 0.5, the frequencies at the bins of $A_c = 0.0$ and $A_c = 1.0$ are about the same for U-shaped distributions and the top of the bell is located at the bin of $A_c = 0.5$ for bell-shaped distributions. On the other hand, when the regional-scale cloud cover TA_c is not 0.5, the top of the bell is at the bin of $A_c = TA_c$ for bell-shaped distributions, and the frequency at the bin of $A_c = 1.0$ is larger (smaller) than that at the bin of $A_c = 0.0$ for U-shaped distributions if TA_c is greater (less) than 0.5. The L- and J-shaped distributions are two special examples of U-shaped distribution when TA_c approaches 0 and 1, respectively (see Burger 1985 for a thorough discussion).

Several authors (e.g., Falls 1974; Burger 1985; Henderson-Sellers and McGuffie 1991; Chang and Coakley 1992, see Karner and Keevallik 1993 for a summary) have studied the approximation of the shape of cloud-cover frequency distributions. For the purpose of this study, the shape is simply described by a shape parameter U defined as

$$U = 0.5[f(1.0) + f(0)] - f(TA_c), \qquad (1)$$

where $f(1.0)$, $f(0)$, and $f(TA_c)$ are the normalized frequencies at the bins of $A_c = 1.0$, $A_c = 0$, and $A_c = TA_c$, respectively. For a U-shaped distribution, the shape parameter U is positive and serves as an estimate of the depth of the U shape. For a bell-shaped distribution, U is negative and its magnitude is a measure of the height of the bell. In this study, $f(TA_c)$ is calculated as the average of the two frequencies in the two bins with A_c's closest to TA_c. For example, when $TA_c = 0.5$, the frequency of the 10th bin (for A_c between 0.45 and 0.50) and that of the 11th bin (for A_c between 0.50 and 0.55) are averaged for $f(TA_c)$. Consequently, the maximum value of $f(TA_c)$ is 0.5, and the minimum value of U is -0.5. Another parameter, the size ratio, is defined as the ratio of cloud size to pixel size:

$$R = \frac{\text{cloud size}}{\text{pixel size}}. \qquad (2)$$

Figure 3 shows, for the case where $TA_c = 0.5$, how

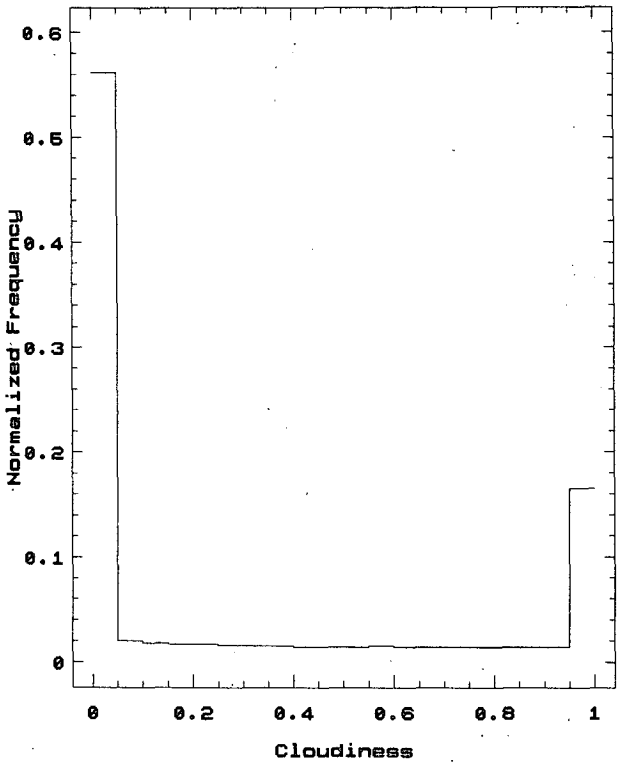

FIG. 2. An example of the pixel-scale cloud-cover normalized frequency distribution. The cloud size is 60. The pixel size is 20. The regional-scale cloud cover is 0.3.

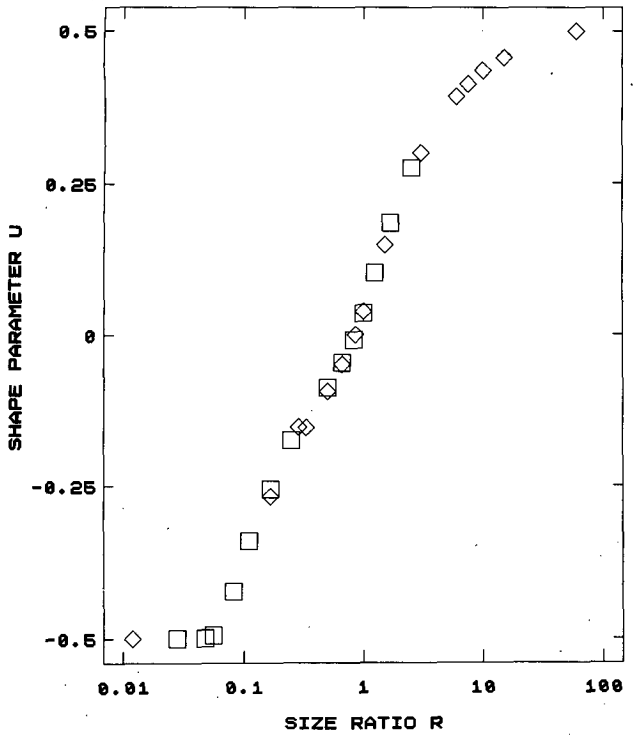

FIG. 3. The relationship between shape parameter U and the ratio R of cloud size to pixel size, for the case where the regional-scale cloud cover is 0.5. Different cloud sizes and pixel sizes are used to provide a variety of size ratios. Squares are for the cases where cloud size is 10. Diamonds are for the cases where cloud size is 60.

shape parameter U depends on size ratio R. Different pixel sizes and cloud sizes are used to provide a variety of size ratios. Figure 3 also shows that shape parameter U depends only on size ratio R; U does not depend on cloud size explicitly, since the U's of different cloud sizes fall into the same curve. Similarly, U does not depend on pixel size explicitly, since different pixel sizes can offer the same U, as long as the size ratios are the same.

As shown in Fig. 3, U increases with increasing R, indicating that the population of cloud-free and overcast pixels increases with increasing R. Here U becomes "saturated" at the maximum value of 0.5 when R is greater than about 20. Once R is large enough and the frequencies are all concentrated at the bins of $A_c = 1.0$ and $A_c = 0.0$, the shape of the frequency distribution will no longer change. Shape parameter U also saturates, in a similar fashion, at the minimum value of -0.5 when R is less than about 0.06. Here U becomes zero when R is about 0.8–0.9 and the frequency distribution is fairly uniform. The relationship in Fig. 3 can be approximated by

$$U = a \log(R) + b, \qquad (3)$$

where $a = 0.435$ and $b = 0.065$. If $R < 0.05$, U is set to -0.5, and if $R > 10$, U is set to 0.5.

For the cases where the regional-scale cloud cover TA_c is not 0.5, Figure 4 shows the dependence of shape parameter U on size ratio R and TA_c. The part of $TA_c > 0.5$ is roughly symmetric to that of $TA_c < 0.5$, since placing a fraction TA_c of cloud-covered area in a cloud-free analysis area is the same as placing a fraction $(1 - TA_c)$ of cloud-free area in an overcast analysis area. Consequently, an L-shaped distribution may have a shape parameter that is the same as that of a J-shaped distribution. The regional-scale cloud cover is therefore a necessary parameter that distinguishes between J- and L-shaped distributions. Figure 4 also shows that U increases with increasing R at all TA_c's. When $R > 0.5$, U also increases with TA_c departure from 0.5. This increase is due to the redistribution of the frequencies between the two wings of the U shape, contributed by partially cloudy pixels, as the relative heights of the two wings change. The rate of increase gets less evident as the size ratio R increases, reducing the frequencies at the bins between the two wings and thus their effects. When $R < 0.17$, U decreases with TA_c departure from 0.5 in a similar fashion.

a. The population of partially cloudy pixels

The dependence of pixel-scale cloud-cover frequency distribution on size ratio, shown in Figs. 3 and 4, can be used to examine the population of partially cloudy covered pixels in the analysis region. Figure 5 shows

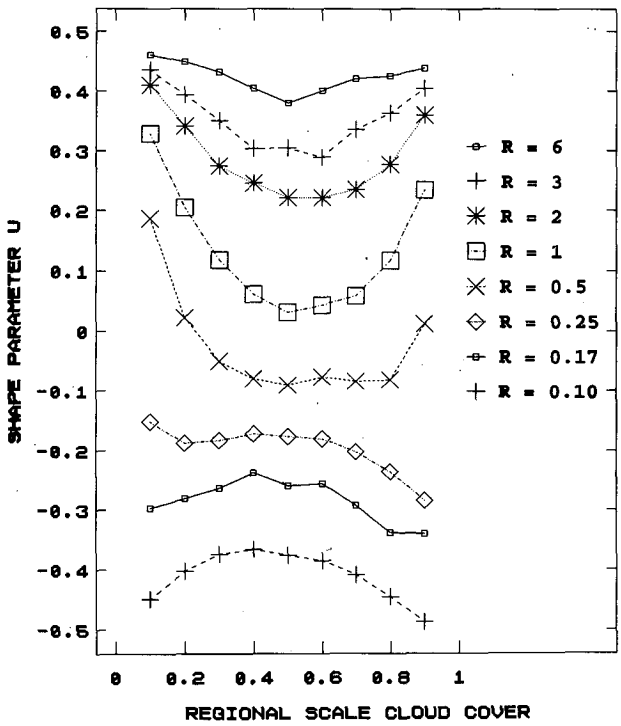

FIG. 4. The relationship between shape parameter U, size ratio R, and regional-scale cloud cover.

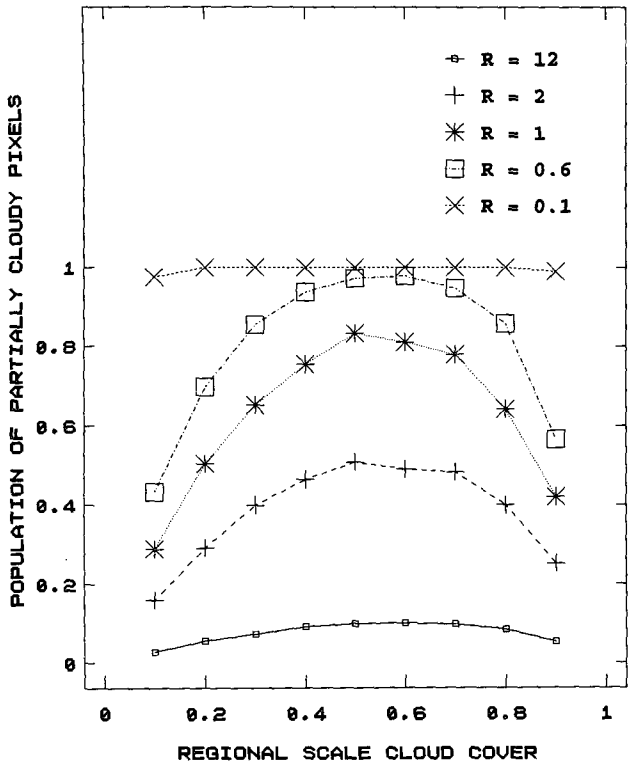

FIG. 5. The relationship between the normalized population of partially cloudy pixels, regional-scale cloud cover, and size ratio R.

that the normalized population of partially cloudy pixels increases with decreasing size ratio. This is because when size ratio decreases, the pixel-scale cloud-cover frequency distribution becomes less U shaped (or more bell shaped), thus the normalized population of the partially cloudy pixels increases. For the case where the regional-scale cloud cover is around 0.5, Fig. 5 shows that the normalized population of partially cloudy pixels is about 0.5 when the size ratio is about 2, which is probably similar to the example given by Chang and Coakley (1993). Chang and Coakley (1993) observed that, for a 60–250-km region, the normalized population of 4–8-km satellite pixels that were partially cloudy was approximately 0.5. Figure 5 also shows that the normalized population of partially cloudy pixels approaches 1 (all pixels are partially cloudy) when the size ratio is less than 0.6. When the size ratio is more than 12, however, the normalized population is less than 0.1, indicating that a threshold method that defines all partially cloudy pixels to be overcast would overestimate the regional-scale cloud cover by no more than 10%. This is consistent with Shenk and Solomonson (1972), who concluded that the size of satellite pixel should be one order of magnitude smaller than the typical cloud size for a threshold method to obtain a regional-scale cloud cover within 10% accuracy. Wielicki and Welch (1986), however, commented that the retrieved regional-scale cloud cover from satellite data is not as sensitive to imager resolution as predicted from Monte Carlo simulations.

Figure 5 implies that, for a certain regional-scale cloud cover, the normalized population of partially cloudy pixels depends only on size ratio. It does not depend explicitly on the size of the analysis region. Chang and Coakley (1992), however, observed that, when regional size changes from 250 to 60 km, the normalized population of partially cloudy pixels becomes larger (Fig. 11 of Chang and Coakley 1992). This discrepancy is probably due to the difference between the cloud field simulated in the Monte Carlo model, where clouds are uniformly distributed, and that in the real world, where clouds are not limited to a uniform distribution (Shenk and Solomonson 1972). In the real world, as the regional scale decreases, there are fewer ways for clouds to be distributed to attain a certain regional-scale cloud cover, thus a smaller region has to have more partially cloudy pixels to achieve a given regional-scale cloud cover (J. Coakley 1994, personal communication). In the simulated cloud field, on the other hand, the way for clouds to be distributed is fixed and, as a result, the normalized populations of partially cloudy pixels are similar for large and small regions.

b. The cloud cover of partially cloudy pixels

The dependence of pixel-scale cloud-cover frequency distribution on size ratio can also be used to examine the average cloud cover of partially cloudy pixels. Molnar and Coakley (1985) and Chang and Coakley (1993) observed that, on average, the cloud cover in partially cloudy pixels is large when the regional-scale cloud cover is large, and when the regional-scale cloud cover is small, the cloud cover in partially cloudy pixels is also small. Figure 6 shows that the average cloud cover of the partially cloudy pixels increases with increasing regional-scale cloud cover. The increase, however, gets less evident as the size ratio increases. This is consistent with the dependence of the shape of pixel-scale cloud-cover frequency distribution on size ratio, shown in Figs. 3 and 4. The smaller the size ratio is, the more concentrated the frequency distribution is at the location of the top of the bell shape and the closer the average cloud cover of partially cloudy pixels is to the regional-scale cloud cover. On the other hand, when size ratio is large, the distribution is U shaped and the part of the frequency distribution contributed by the partially cloudy pixels is close to a uniform distribution (Chang and Coakley 1992). The average cloud cover of such pixels, thus, is much less dependent on the regional cloud cover.

The regional-scale cloud cover can be calculated, as suggested by Molnar and Coakley (1985), from the normalized populations of cloud-free and overcast pixels [Eq. (5) of Molnar and Coakley 1985]. Figure 7 shows that the calculated regional-scale cloud cover

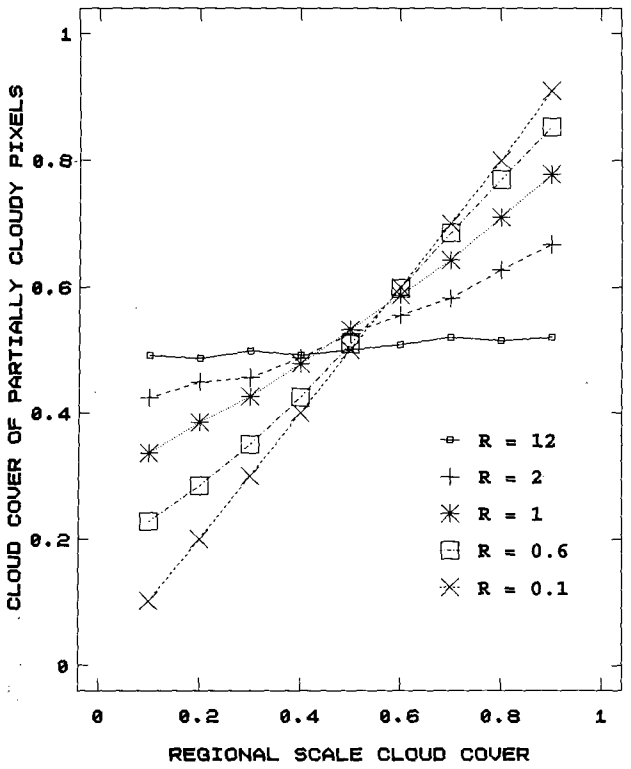

FIG. 6. The dependence of the average cloud cover of partially cloudy pixels on regional-scale cloud cover, for different size ratios (R's).

generally agrees with the true regional-scale cloud cover in the Monte Carlo model. The disagreement at small size ratios is caused in the simulations, where, when the size ratio becomes small, the normalized population of partially cloudy pixels approaches 1 and those of cloud-free and overcast pixels approach zero (Fig. 5), forcing the formula of Molnar and Coakley (1985) to take the value of 0.5 as the regional-scale cloud cover. In other words, sizable populations of cloud-free and overcast pixels are necessary to use the method of Molnar and Coakley (1985). Figure 7 also shows that, although the average cloud cover of partially cloudy pixels is insensitive to the regional-scale cloud cover at large size ratios (Fig. 6), the method of Molnar and Coakley (1985) gives reasonable results, since, at such size ratios, partially cloudy pixels have a small normalized population (Fig. 5) and thus little impact.

4. Grid-scale cloud-cover frequency distribution

The normalized frequency distribution of the cloud covers of all the grids in the analysis region can also be histogrammed in the same fashion in which the pixel-scale cloud-cover frequency distribution was histogrammed, as depicted in Fig. 2. It is logical that the dependence of grid-scale cloud-cover frequency distribution on the ratio of cloud size to grid size is the same as that of pixel-scale cloud-cover frequency distribution on the ratio of cloud size to pixel size. In the Monte Carlo model, there is practically no difference between a grid and a pixel, except that grid size is much larger than pixel size. In other words, once the size ratio is defined to be the ratio of cloud size to grid size [cf. Eq. (2)], the shape parameter of a grid-scale cloud-cover frequency distribution, defined by Eq. (1), also depends on the size ratio in the way shown in Figs. 3 and 4. The form of a grid-scale cloud-cover frequency distribution, therefore, also changes from U shape to bell shape when the ratio of cloud size to grid size decreases, as noted by Falls (1974). In addition, the shape of a grid-scale cloud-cover frequency distribution is independent of pixel size. The cloud cover in each grid is always the ratio of the number of overcast resolution elements to the number of total resolution elements in the grid, regardless of the size of the pixel through which the grid-scale cloud cover is accumulated.

The grid-scale cloud-cover frequency distribution obtained from the Monte Carlo model can be compared to those obtained from a cloud retrieval algorithm. A typical cloud retrieval algorithm is the threshold method that makes a cloud/no-cloud decision to each pixel, like that used in ISCCP (International Satellite Cloud Climatology Project; Schiffer and Rossow 1984; Rossow and Schiffer 1991). Another typical al-

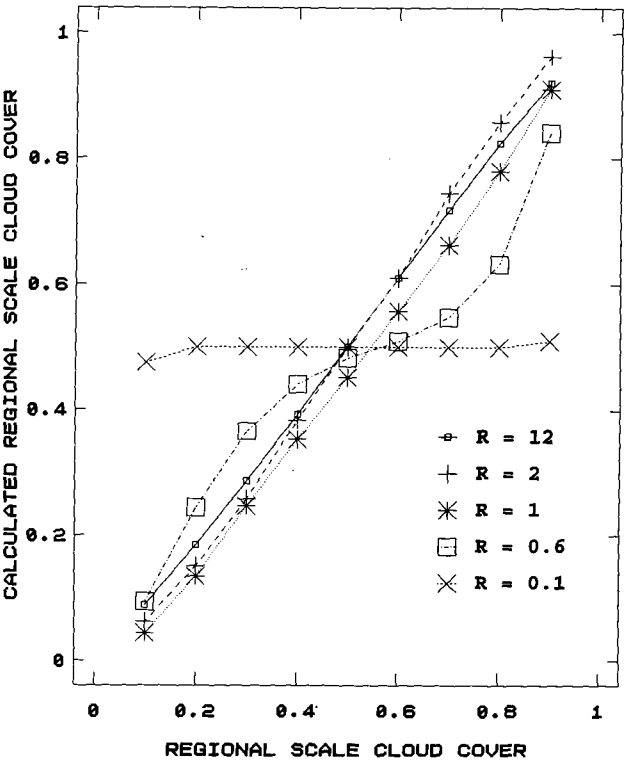

FIG. 7. Comparison between the regional-scale cloud cover calculated from the method suggested by Molnar and Coakley (1985) and the true regional-scale cloud cover, for different size ratios (R's).

gorithm is the method that assigns a fractional cloud cover of 0.5 to partially cloudy pixels, like that used in CLAVR (clouds from AVHRR) phase I (Stowe et al. 1991). The method that assigns a fractional cloud cover of 0.5 to partially cloudy pixels is referred to as the "assignment" method for convenience. Comparisons have been made between cloud covers retrieved from different algorithms (e.g., Rossow et al. 1985; Wielicki and Parker 1992; Hou et al. 1993; Rossow et al. 1993). Comparing grid-scale cloud-cover frequency distributions may also provide insights into cloud retrieval algorithms.

A threshold method and an assignment method are simulated, as shown below, to illustrate the impact of using these methods on grid-scale cloud-cover frequency distributions. The regional-scale cloud cover is fixed at 0.5 for simplicity. The results are applicable to global cloud-cover frequency distributions, since the global cloud cover is about 0.5 (Stowe et al. 1989). It should be noted that the discussions on the two methods are aimed to be illustrative, not conclusive.

a. Shape parameter obtained using the threshold method

A "cloud-cover threshold" is used in the simulated threshold method. Each pixel is reassigned a cloud cover of zero (cloud free), if its cloud cover is less than the cloud-cover threshold, or a cloud cover of 1 (overcast), if its cloud cover exceeds the cloud-cover threshold. The overestimation in the regional-scale cloud cover obtained using a threshold has been discussed by many authors (e.g., Shenk and Solomonson 1972; Coakley and Bretherton 1982; Wielicki and Welch 1986; Wielicki and Parker 1992; Chang and Coakley 1993). To isolate the impact of using a threshold method on grid-scale cloud-cover frequency distribution, the cloud-cover threshold is set at 0.5 so that the regional-scale cloud cover, accumulated after using the threshold method, is the same as the true regional-scale cloud cover. The application of the cloud/no-cloud threshold changes the pixel-scale cloud cover in the Monte Carlo model. The grid-scale cloud covers obtained using the simulated threshold method will be different from those obtained from original Monte Carlo simulations. In addition, pixel size now influences the results, since, in the simulated threshold method, the grid-scale cloud covers are accumulated from pixels with reassigned cloud covers.

Figure 8 shows the relationship between the shape parameter of the frequency distribution of grid-scale cloud covers, obtained using the simulated threshold method, and the ratio of cloud size to grid size. Cases of different pixel size to grid size ratios are included to reflect the impact of pixel size. For comparison, results from original Monte Carlo simulations are also included. They are referred to, hereafter, as the results from "Monte Carlo" simulations for simplicity.

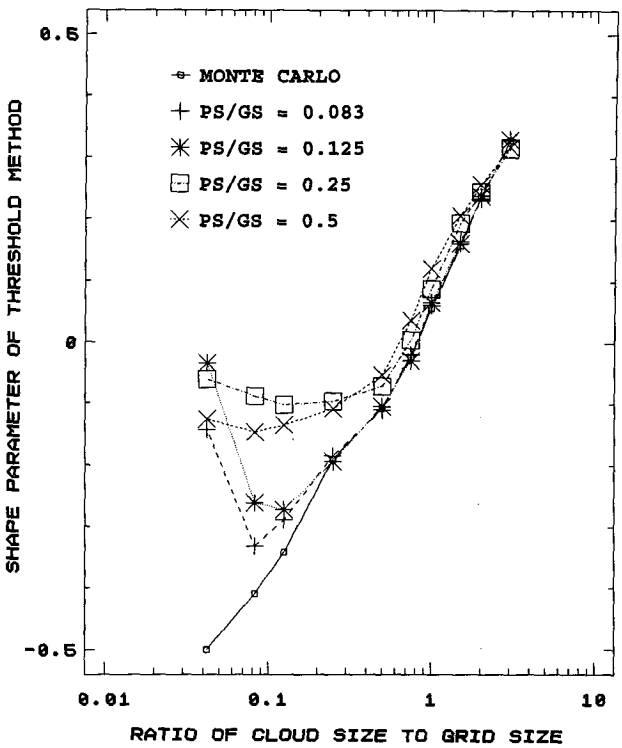

FIG. 8. The relationship between shape parameter, the ratio of cloud size to grid size, and the ratio of pixel size to grid size (PS/GS) for grid-scale cloud-cover frequency distribution obtained using a threshold method and that obtained from Monte Carlo simulations. The regional-scale cloud cover is 0.5.

Figure 8 suggests that, in comparison with the results from Monte Carlo simulations, the shape parameter of the grid-scale cloud-cover frequency distribution obtained using the simulated threshold method tends to be more U shaped, since the application of the cloud/no-cloud threshold to each pixel makes clouds more contiguous, leading to a magnified cloud size. For example, when cloud size is smaller than pixel size (subgrid cloudiness), all clouds are either neglected or reassigned a size equal to pixel size, leading to an enlargement of cloud size. As shown in Fig. 8, a significant difference between the results obtained using the threshold method and those from Monte Carlo simulations appears when the ratio of cloud size to pixel size is smaller than 2. For example, for the case where the ratio of pixel size to grid size is 0.25, a considerable difference appears when the ratio of cloud size to grid size is less than 0.5 (i.e., the ratio of cloud size to pixel size is less than 2). For the case where the ratio of pixel size to grid size is 0.125, a large difference occurs when the ratio of cloud size to pixel size is also less than 2 (the ratio of cloud size to grid size is less than 0.25). Figure 8 also shows, however, that the shape parameter obtained using the threshold method is close to that from Monte Carlo simulations when the ratio of cloud size to pixel size is greater than 2.

b. Shape parameter obtained using the assignment method

In the simulated assignment method, partially cloudy pixels (pixels having a cloud cover between the values of 0.05 and 0.95) are reassigned a cloud cover of 0.5. The regional-scale cloud cover, as a result, remains about the same as the true regional-scale cloud cover. Similar to the case of the simulated threshold method, the grid-scale cloud covers obtained using the simulated assignment method will be different from those obtained from Monte Carlo simulations. Also, pixel size now influences the results.

Figure 9 shows, along with the results from Monte Carlo simulations, the relationship between the shape parameter of the grid-scale cloud-cover frequency distributions obtained using the assignment method, the ratio of cloud size to grid size, and the ratio of pixel size to grid size. In comparison with the results from Monte Carlo simulations, the shape parameter of the grid-scale cloud-cover frequency distribution obtained using the simulated assignment method tends be less U shaped. As discussed in section 3b, there is a link between the average cloud cover of partially cloudy pixels and the cloud cover in the larger area where such pixels are examined. The larger area, here, is the area of a grid. For the cases where cloud size is smaller than pixel size, almost all pixels are partially cloudy and the pixel-scale cloud-cover frequency distributions in the grids are bell shaped. The tops of the bells may locate at different cloudiness bins in different grids. The assignment method, however, changes the form of the pixel-scale cloud-cover frequency distribution in each grid from bell shaped to a single spike at the bin of cloudiness equal to 0.5, forcing the cloud cover of each grid to approach 0.5. Hou et al. (1993) noted that, because of the assigned fractional cloud cover of 0.5 to all partially cloudy pixels, the frequency distribution of the cloud covers of the equal longitude–latitude grid boxes in the global mapping of CLAVR phase I is biased toward 50% cloudiness. Similar to the case of the simulated threshold method shown in Fig. 8, Fig. 9 also shows that, when the ratio of cloud size to pixel size is greater than 2, the shape parameter of the grid-scale cloud-cover frequency distribution obtained using the assignment method is close to that obtained from Monte Carlo simulations, except for the case where the ratio of pixel size to grid size is 0.5.

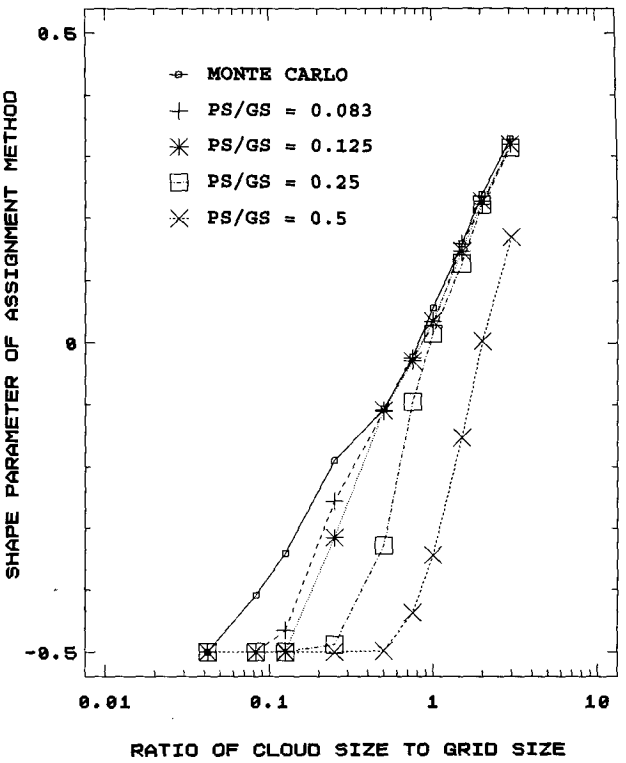

FIG. 9. The relationship between shape parameter, the ratio of cloud size to grid size, and the ratio of pixel size to grid size (PS/GS) for grid-scale cloud-cover frequency distribution obtained using the assignment method and that obtained from Monte Carlo simulations. The regional-scale cloud cover is 0.5.

c. Cloud size estimation

Cloud size estimation is necessary for obtaining cloud size distribution, which may become an essential ingredient of future cloud-cover parameterizations used in climate models (Coakley and Bretherton 1982). Many authors have reported their work on cloud size retrieval (e.g., Plank 1969; Hughes and Henderson-Sellers 1983; Wielicki and Welch 1986; Kuo et al. 1993). The dependence of grid-scale cloud-cover frequency distribution on size ratios, discussed in the previous sections, suggests that cloud size can be estimated from observed grid-scale cloud-cover frequency distribution. Especially, for cases where the regional-scale cloud cover is 0.5, Figs. 8 and 9 can be used to approximate the cloud size from the shape parameter of the grid-scale cloud-cover frequency distribution obtained from a cloud retrieval algorithm, which, like the ISCCP or CLAVR phase I algorithm, uses a threshold method or an assignment method. Owing to the fact that a cloud field in the real world may contain clouds of different layers and/or types, the single layer in Monte Carlo simulations is considered the "effective" cloud layer, and the single cloud size is considered the "effective" cloud size. Whether or not the effective cloud size is linked to a parameter in a realistic cloud size distribution, it is an index for distinguishing cloud systems with distinctly different cloud sizes. There appears to be no advantage in using a cloud size distribution instead of a single cloud size. In addition, with the overlap between clouds, the simulated cloud field contains, to a certain degree, a built-in cloud size distribution.

Figure 10 is from Hou et al. (1993). It shows the global frequency distributions of the 1° latitude–lon-

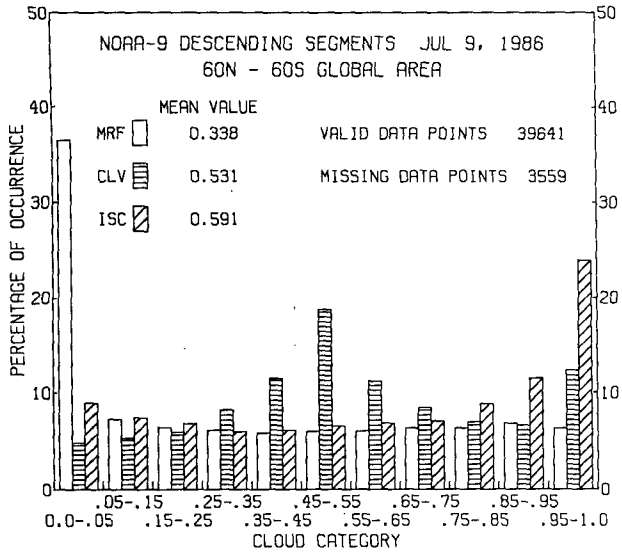

FIG. 10. Frequency distributions of cloud covers of 1° equal latitude–longitude grid boxes between 60°N and 60°S on 9 July 1986 obtained from ISCCP (ISC), CLAVR phase I (CLV), and NMC's Medium Range Forecast Model (MRF) (from Hou et al. 1993).

gitude grid box cloud covers from ISCCP and CLAVR phase I. The results from the forecast by a research version of NMC's Medium Range Forecast (MRF) Model (Kanamitsu 1989), also shown in Fig. 10, are not used. The effective cloud size can be assumed to be the same for ISCCP and CLAVR phase I, since both algorithms were applied to the same cloud field (the globe between 60°N and 60°S) on the same day. The total cloud covers are close to 0.5 (0.59 for ISCCP; 0.53 for CLAVR phase I), thus the results in Figs. 8 and 9 are applicable. The shape parameters of the frequency distributions in Fig. 10 can be calculated using Eq. (1), which are $U = 0.10$ for ISCCP and $U = -0.11$ for CLAVR phase I. According to Hou et al. (1993), the cloud covers of ISCCP were from 250-km equal-area grids, transformed into 2.5° equal-angle grids, and then upgraded into 1° equal-angle grids. Upgrading grid size does not change the shape of the normalized frequency distribution of the grid-scale cloud covers, since the cloud covers in the finer grids inherit those in the coarser ones. The grid size of ISCCP to be used in the analysis here should be 250 km at nadir. On the other hand, the cloud covers of CLAVR phase I were from 0.5° equal-angle grids, degraded into 1° equal-angle grids. Degrading grid size decreases the ratio of cloud size to grid size. The grid size of CLAVR phase I used in the analysis here should be the size of the degraded equal-angle grids, which is about 100 km at nadir. Consequently, the ratio of pixel size to grid size is less than 0.083 (the satellite pixel size is 4–8 km) for both algorithms. As shown in Figs. 8 and 9, for the part of $U > -0.11$, the curves for the cases where the ratio of pixel size to grid size is less than 0.083 are very close to that from Monte Carlo simulations. The results from Monte Carlo simulations in these figures are therefore used to estimate the ratio of effective cloud size to grid size from the calculated shape parameters. The ratios are about 1.0 for ISCCP and about 0.5 for CLAVR phase I. The effective cloud size is thus estimated to be about 250 km for ISCCP and about 50 km for CLAVR phase I. The inconsistency shown in the two different effective cloud sizes obtained from the same cloud field is significant.

The possible sources of the inconsistency are explained as the following. First, as discussed in section 3a, there is a considerable difference between the cloud field simulated in the Monte Carlo model and that in the real world. While the clouds in the simulated cloud field are limited to a uniform distribution, those in a real cloud field can be distributed in many ways. The larger the region is, the more ways there will be. The clouds in a real cloud field can be distributed in such a way that clouds are concentrated (not necessarily clustered) in some areas, leaving other extensive areas cloud-free (Shenk and Solomonson 1972; also refer to Zhu et al. 1992). Such extensive cloud-free areas make a "permanent" contribution at the bin of $A_c = 0$ in the grid-scale cloud-cover frequency distribution, so that when the grid size increases, the form of the grid-scale cloud-cover frequency distribution will not change from U shape to bell shape as fast as predicted by the Monte Carlo model. It is possible that, in the example shown in Fig. 10, the larger grid size of ISCCP did not reduce the shape parameter as much as predicted in Fig. 8, leading to an overestimated effective cloud size. For CLAVR phase I, however, this effect is unlikely to be significant, since the conservative clear-sky tests will probably keep the extensive cloud-free area from being recognized. Second, cloud edges in satellite data have greater spatial structure than those simulated in the Monte Carlo model, causing a larger number of partially cloudy pixels (Wielicki and Welch 1986). In addition, pixels overcast by clouds of different emissivities or layers can also be given a cloud cover of 0.5 in CLAVR phase I (Stowe et al. 1991). Consequently, the threshold method and the assignment method simulated here underestimate both the overestimation and underestimation in the shape parameters obtained from ISCCP and CLAVR phase I, respectively. The overestimation and underestimation are basically caused by the cloud cover reassignment to partially cloudy pixels. Third, different algorithms use different tests that define clouds. A pixel defined as cloud free in one algorithm may be defined as overcast in another algorithm. Consequently, the effective cloud size will be different from one algorithm to another. Finally, the cloud-cover frequency distributions in Fig. 10 were from equal latitude–longitude grid boxes, not from the equal-sized grids required in the Monte Carlo model.

5. Conclusions

The form of a pixel-scale cloud-cover frequency distribution, described by a shape parameter U, is found to be a simple function of size ratio, defined as the ratio of cloud size to pixel size. The form changes from U shape to bell shape when the size ratio decreases. It becomes uniform when the size ratio is about 0.8–0.9, for the case when the regional scale cloud cover is 0.5.

The normalized population of partially cloudy pixels increases with decreasing size ratio. The regional cloud cover obtained using a threshold is expected to be within 10% accuracy when size ratio is larger than 12. When size ratio is small, the average cloud cover of partially cloudy pixels increases with increasing regional-scale cloud cover. When the ratio becomes large, the average cloud cover becomes insensitive to regional-scale cloud cover. The formula suggested by Molnar and Coakley (1985) is found to give good estimates of regional-scale cloud covers from the normalized populations of cloud-free and overcast pixels.

In comparison with the results from Monte Carlo simulations, the grid-scale cloud-cover frequency distributions obtained using a threshold method tends to be more U shaped, and that obtained using a method that assigns 50% cloudiness to partially cloudy pixels tends to be more bell shaped, especially for subgrid cloudiness. When the ratio of cloud size to pixel size is greater than 2, the shape parameters obtained using these methods are close to those from Monte Carlo simulations.

An example has been shown to estimate the effective cloud size from the grid-scale cloud-cover frequency distributions of ISCCP and CLAVR phase I. The estimate is biased primarily due to the difference between the cloud field simulated in the Monte Carlo model, where clouds are uniformly distributed, and that in the real world, where clouds are not necessarily uniformly distributed. It is noted that, in a real cloud field where clouds are not uniformly distributed, the grid-scale cloud-cover frequency distribution may also depend on grid size. Parameterizations on how clouds are distributed in a real cloud field are recommended.

Acknowledgments. This work is through the UCAR Visiting Scientist Program at NOAA Science Center, Washington, D.C. The author wishes to thank Dr. P. A. Davis for his insightful advice, and Drs. L. L. Stowe, Yu-Tai Hou, C. G. Justus, and G. Ohring for their helpful comments. Especially, the author wishes to thank Dr. J. A. Coakley and the two anonymous reviewers, whose comments brought significant improvement to this paper.

REFERENCES

Burger, C. F., 1985: World atlas of total sky cover. Environmental Resource Paper 927, AFGL-TR-85-0198, Air Force Geophysics Laboratory, Hanscom Air Force Base, MA, 112 pp.

Chang, F.-L., and J. A. Coakley Jr., 1992: Estimating errors in fractional cloud cover obtained with infrared threshold methods. *J. Geophys. Res.*, **98,** 8825–8839.

Coakley, J. A., Jr., and F. P. Bretherton, 1982: Cloud cover from high-resolution scanner data: Detecting and allowing for partially filled fields of view. *J. Geophys. Res.*, **87,** 4917–4932.

Falls, L. W., 1974: The beta distribution: A statistical model for world cloud cover. *J. Geophys. Res.*, **79,** 1261–1264.

Henderson-Sellers, A., and K. McGuffie, 1991: An investigation of the Burger distribution to characterize cloudiness. *J. Climate,* **4,** 1181–1209.

Hou, Y.-T., K. A. Campana, K. E. Mitchell, S.-K. Yang, and L. L. Stowe, 1993: Comparison of an experimental NOAA/AVHRR cloud dataset with other observed and forecast cloud datasets. *J. Atmos. Oceanic Technol.,* **10,** 834–849.

Hughes, N. A., and A. Henderson-Sellers, 1983: The effect of spatial and temporal averaging on sampling strategies for cloud amount data. *Bull. Amer. Meteor. Soc.,* **64,** 250–257.

Kanamitsu, M., 1989: Description of the NWC global data assimilation and forecast system. *Wea. Forecasting,* **4,** 335–342.

Karner, O., and S. Keevallik, 1993: *Effective Cloud Cover Variations.* Deepak Publishing, 210 pp.

Kuo, K.-S., R. M. Welch, and R. C. Weger, 1993: The three-dimensional structure of cumulus clouds over the ocean: 1. Structure analysis. *J. Geophys. Res.,* **98,** 20 685–20 711.

Molnar, G., and J. A. Coakley Jr., 1985: Retrieval of cloud cover from satellite imagery data: A statistical approach. *J. Geophys. Res.,* **90,** 12 960–12 970.

Plank, V. G., 1969: The size distribution of cumulus clouds in representative Florida populations. *J. Appl. Meteor.,* **8,** 46–67.

Rossow, W. B., and R. A. Schiffer, 1991: ISCCP cloud data product. *Bull. Amer. Meteor. Soc.,* **72,** 2–20.

——, F. Mosher, E. Kinsella, A. Arking, M. Desbois, E. Harrison, P. Minnis, E. Ruprecht, G. Seze, C. Simmer, and E. Smith, 1985: ISCCP cloud algorithm intercomparison. *J. Climate Appl. Meteor.,* **24,** 877–903.

——, A. W. Walker, and L. C. Garder, 1993: Comparison of ISCCP and other cloud amounts. *J. Climate,* **6,** 2394–2418.

Schiffer, R. A., and W. B. Rossow, 1984: The International Cloud Climatology Project: The first project of the World Climate Research Programme. *Bull. Amer. Meteor. Soc.,* **64,** 779–784.

Shenk, W. E., and V. V. Solomonson, 1972: A simulation study exploring the effects of sensor spatial resolution on estimates of cloud cover from satellites. *J. Appl. Meteor.,* **11,** 214–220.

Stowe, L. L., H. Y. M. Yeh, T. F. Eck, C. G. Wellemeyer, H. L. Kyle, and the *Nimbus-7* Cloud Data Processing Team, 1989: *Nimbus-7* global cloud climatology. Part II: First year results. *J. Climate,* **2,** 671–709.

——, E. P. McClain, R. Carey, P. Pellegrino, G. Gutman, P. Davis, C. Long, and S. Hart, 1991: Global distribution of cloud cover derived from NOAA/AVHRR operational satellite data. *Adv. Space Res.,* **11,** 51–54.

Wielicki, B. A., and R. M. Welch, 1986: Cumulus cloud properties derived using Landsat satellite data. *J. Climate Appl. Meteor.,* **25,** 261–276.

——, and L. Parker, 1992: On the determination of cloud cover from satellite sensors: The effect of sensor spatial resolution. *J. Geophys. Res.,* **97,** 12 799–12 823.

Zhu, T., J. Lee, R. C. Weger, and R. M. Welch, 1992: Clustering, randomness, and regularity in cloud fields: 2. Cumulus cloud fields. *J. Geophys. Res.,* **97,** 20 537–20 558.